A NONLINEAR MODEL TO CALCULATE THE STRESSED STATE OF A CENTER-WOUND ROLL

by

C. A. Piper

3M Company
St. Paul, MN, U.S.A.

ABSTRACT

This work develops a model to calculate the stressed state of center-wound rolled webs, such as film, paper, or foil. The model is built on a lesser known linear model developed by Umanskii and accounts for the nonlinear stress-strain relationship of the roll in the radial direction as determined from uniaxially compressing a stack of the material. The main cause of this nonlinear behavior is inter-layer air entrapment and web surface roughness. The more popular published linear model developed by Altmann has been extended by Hakiel to include the roll's nonlinear radial stress-strain relationship. However, recent published work shows the radial stresses predicted by Hakiel to be significantly greater than measured data using calibrated pull tabs for some webs.

Results from this nonlinear model are compared to published measured in-roll radial stress data for three materials: PET, newsprint, and bond paper. After eliminating the softest portion of the stack test data, the model predicted in-roll radial stresses that agree well with the experimental data for PET. The predicted in-roll radial stresses were less than the experimental data for both papers. However, results from the Hakiel model and the new nonlinear model were found to provide bounds for the experimental data for paper.

NOMENCLATURE

a	:Inner radius of hub
b	:Outer radius of hub
c	:Outer radius of wound roll
r	:Radial position
u	:radial displacement
ε_θ	:In-roll circumferential strain
ε_r	:In-roll radial strain

σ_θ :In-roll circumferential stress

σ_r :In-roll radial stress

σ_w :Winding stress, which is the winding tension divided by the web's cross-sectional area

E_c :Effective compliance of the core taken as an isotropic cylinder

E_r :Modulus of elasticity of a linear roll in the radial direction or the instantaneous slope of the stress-strain curve of a nonlinear stack.

E_θ :Modulus of elasticity of wound roll in the circumferential direction

E_h :Modulus of elasticity of the core material

υ_h :Poisson's ratio of the core material

$\upsilon_{\theta r}$:Poisson's ratio of web in the circumferential direction. Ratio of radial strain to circumferential strain for an element under pure circumferential stress, assumed constant throughout the roll

$\upsilon_{r\theta}$:Poisson's ratio of web in the radial direction. Ratio of circumferential strain to radial strain for an element under pure radial strain, assumed constant throughout the roll

INTRODUCTION

A convenient and common way to store web materials is in the form of a wound roll. Maintaining quality of the wound roll is important to maintaining overall quality of the product, and roll quality depends on the residual stresses in the roll. Center-winding is a common winding process where the motor torque is applied to the roll through the core which is mounted on a spindle. In center-winding, no external forces are applied to the roll's outer surface.

Currently, roll quality is optimized by conducting designed experiments. This is not a trivial task and is costly as both a trained technician and machine time are required. A mathematical model to predict the stressed state of center-wound rolls is valuable in optimizing roll quality efficiently. Such a model would reduce the expense of providing high quality rolls in which roll defects are minimized and product performance is improved.

Some of the early work modeled the roll as an isotropic cylinder with material properties all constant throughout the roll. Later models viewed the roll as an orthotropic material due to the roll being softer in the radial direction. The stress-strain relationship in the radial direction is determined from uniaxially compressing a stack of material. Such tests reveal the roll's radial stress-strain behavior to be nonlinear. This is attributed to inter-layer entrapped air and material surface roughness (Forrest, 1993).

This work presents a nonlinear model that predicts in-roll radial stresses that agree well with published experimental data for PET rolls. However, the paper results are interesting in that in-roll radial stresses predicted by an earlier model of Hakiel (1985) and the new model were found to bound the experimentally determined stresses.

First the stack test is discussed, then the nonlinear model is formulated. The solution technique for the in-roll stresses is then discussed, and finally the stresses from the model are compared to experimental radial stress data obtained from Swanson (1991).

STACK TESTS

A stack test is conducted to determine the material's stress-strain relationship in the radial direction under pure radial stress. Figure 1 shows a stack test configuration. The strain vs. stress data from a stack test (conducted by Swanson, 1991) on PET is shown in Fig. 2. This strain vs. stress relationship can be expressed as:

$$\varepsilon = g(\sigma) \tag{1}$$

Similar strain vs. stress relationships from stack tests on newsprint and bond paper are presented by Piper (1994). Compressive strain and pressure are the negative of radial strain and radial stress respectively in Fig. 2. Superimposed on each graph is the fitted curve of the form in Eq. (2).

An analytical expression is needed to determine the function $g(\sigma)$ that characterizes a stack's strain vs. stress behavior. The most convenient solution is a single function $g(\sigma)$ that fits the stack test data.[1] The best fit was obtained from a combination of exponential functions and a linear function.[2] The function is:

$$\varepsilon = k_1\sigma - k_2(1 - e^{k_3\sigma}) - k_4(1 - e^{k_5\sigma}) \tag{2}$$

The two exponential terms in Eq. (2), $k_2(1 - e^{k_3\sigma})$ and $k_4(1 - e^{k_5\sigma})$, describe the sharp rise and transition region of the curve shown in Fig. 2. However, as is characteristic of an exponential function, each exponential term reaches a steady state value. For the first exponential term in Eq. (2), $k_2(1 - e^{k_3\sigma})$, the steady state value is k_2. The constant k_3 determines how fast the function rises to the steady state value. The linear term in Eq. (2) is included to fit the final linear region.

The least squares method is utilized to determine the constants k_1 through k_5 of function $g(\sigma)$ in Eq. (2) that best fits the stack test data. Since the data and Eq. (2) is nonlinear, the constants are determined using a nonlinear least squares fit.

NONLINEAR MODEL FORMULATION

This section develops a non-linear winding model built from Umanskii's (1978) linear orthotropic model. The model incorporates the roll's non-linear radial stress-strain relationship as determined from a stack test. First the model assumptions are presented, then the stress equilibrium equation and strain-displacement relationships are utilized. Then the resulting second order differential equation and boundary conditions of the roll are presented.

The model's assumptions are the same as Altmann's (1968) and Umanskii's (1978) except that the radial stress-strain relationship is assumed to be nonlinear as determined from uniaxially compressing a stack of material.

Equilibrium of a differential element of a stressed cylinder gives:

---

[1] A cubic spline would also probably work, but the spline segment used would depend on the current σ value.

[2] A constant term was intentionally omitted in performing the least squares fit to force the curve to pass through the origin.

$$r\frac{d\sigma_r}{dr} + \sigma_r - \sigma_\theta = 0 \tag{3}$$

This is the standard equilibrium equation in polar form. The circumferential and radial strains are as follows:

$$\varepsilon_\theta = \frac{u}{r} + \frac{\sigma_w}{E_\theta} \tag{4}$$

and

$$\varepsilon_r = \frac{du}{dr} - \upsilon_{\theta r}\frac{\sigma_w}{E_\theta} \tag{5}$$

where σ_w is the original winding stress of that element when it first entered the roll. The second (σ_w) term in Eq. (4) is the circumferential pre-strain of each ring added to the roll as presented in Umanskii's (1978) original work. Note that a radial pre-strain is included in Eq. (5) which was not included in Umanskii's (1978) original work.[3] This is included because the entering web under the winding stress will be strained in the radial direction also due to the Poisson effect.

The stress-strain relationships used for an orthotropic material in polar coordinates are:

$$\varepsilon_r = g(\sigma_r) - \upsilon_{\theta r}\frac{\sigma_\theta}{E_\theta} \tag{6}$$

$$\varepsilon_\theta = \frac{\sigma_\theta}{E_\theta} - \frac{\upsilon_{\theta r}}{E_\theta}\sigma_r \tag{7}$$

The function, $g(\sigma_r)$, is used because it describes the stress-strain relationship of the roll under pure radial stress. For a linear orthotropic material, $g(\sigma_r)$ would be replaced by σ_r/E_r. Equation (6) equates the roll's radial strain to the sum of two terms. The first is the material's radial strain due to pure radial stress. The second is the material's transverse (radial) strain under pure hoop stress. The second term is the classical Poisson effect where a material under uniaxial stress has a transverse strain directly proportional to the normal strain.

Equation (7) equates the roll's hoop strain to the sum of two terms also. The first term is the material's hoop strain while under pure hoop stress. The second term is the material's hoop strain while under pure radial stress. This is not the classical Poisson effect, because the second term is not proportional to the radial strain from the stack test. This is because while the material is undergoing large strains due to inter-layer air and surface roughness, a transverse strain proportional to the normal strain would not be expected. It is more realistic to expect the transverse strain to be proportional to the

[3]Computer simulations show that including the radial pre-strain changes the hoop stresses by as much as 20 %.

radial stress, not the radial strain. The constant of proportionality is obtained by assuming a linear, orthotropic material obeying Maxwell's reciprocal theorem.[4]

The differential equation developed for the wound roll with a non-linear radial stress-strain relationship is expressed in terms of radial stress. The derivation of the differential equation in radial stress begins by rearranging the stress equilibrium equation (Eq. 3) and differentiating with respect to r:

$$\frac{d\sigma_\theta}{dr} = r\frac{d^2\sigma_r}{dr^2} + 2\frac{d\sigma_r}{dr} \tag{8}$$

The Poisson's ratio term, $\upsilon_{\theta r}$, is assumed to be constant. Combining Eqs. (4) and (7) and differentiating with respect to r gives:

$$\frac{du}{dr} = \frac{u}{r} + \frac{r}{E_\theta}\left[\frac{d\sigma_\theta}{dr} - \upsilon_{\theta r}\frac{d\sigma_r}{dr} - \frac{d\sigma_w}{dr}\right] \tag{9}$$

Combining Eqs. (3) through (9) gives:

$$\frac{d^2\sigma_r}{dr^2} + \frac{3}{r}\frac{d\sigma_r}{dr} + \frac{1}{r^2}\sigma_r - \frac{E_\theta}{r^2}g(\sigma_r) = \frac{1+\upsilon_{\theta r}}{r^2}\sigma_w + \frac{1}{r}\frac{d\sigma_w}{dr} \tag{10}$$

Equation (10) is the second order differential equation that must be solved to obtain the internal stress field of the roll. In order to solve this equation for the radial stress, two boundary conditions are needed.

The first boundary condition is at the core's outer radius. This states that the core's outer surface deflects linearly with the radial stress applied from the roll (Timoshenko, 1967), or:

$$u = \frac{b\sigma_r}{E_c} \qquad \text{when } r = b \tag{11}$$

This boundary condition at the core can be written as (Piper, 1994):

$$\frac{d\sigma_r}{dr} = \frac{1}{b}\left[\left(\frac{E_\theta}{E_c} + \upsilon_{\theta r} - 1\right)\sigma_r + \sigma_w\right] \qquad \text{when } r = b \tag{12}$$

The other boundary condition is at the outer surface of the wound roll:

$$\sigma_r = 0 \qquad \text{when} \quad r = c \tag{13}$$

These two boundary conditions can be used to solve the second order differential equation for the radial stress. The next section explains how the differential equation is solved using these boundary conditions.

SOLUTION TECHNIQUE

Equation (10) is a nonlinear second order differential equation which does not have a closed form solution. Therefore, a numerical method is employed. Since one

---

[4]Equation (7) was proposed by M.R. Huble, a Ph.D. candidate in the Mech. Eng. Dept. of the University of Minnesota. It is also discussed in her Ph.D. thesis, which is not yet published at the time of this writing.

boundary condition is at the core (Eq. 12) and the other at the outer surface (Eq. 13), this is a boundary-value problem. The specific numerical methods and the rationale for selecting them are briefly discussed here.

Solution methods for boundary-value problems fall into three general categories. The first is a technique that reduces the problem to solving multiple initial-value problems. This is known as the "Shooting Method." In this method, the initial value that satisfies the known boundary condition is solved for iteratively using an optimization scheme. The second general method involves writing the differential equation in a finite difference form. This results in a finite difference equation at each of a series of discrete points. The resulting system of equations can then be solved using standard methods. This is known as the Finite Difference Method. The third method divides the domain into subintervals or elements connected at points called nodes. The separate element equations are combined or "assembled" to give a set of equations which can be solved for the nodal values once the equations are adjusted to meet the boundary conditions. This method is the Finite Element Method. These methods are treated extensively in numerical methods texts such as Gerald and Wheatley (1994).

Since a single differential equation is available to quantify the stresses throughout the roll (Eq. 10), the complexity of a finite element solution was not justified. Furthermore, when the original differential equation is non-linear, the finite difference method yields a system of non-linear equations. In these cases Gerald and Wheatley (1994) state that the shooting method is normally preferred. Therefore, the shooting method was used to solve the boundary-value problem.

Equations (10), (12), and (13) describe the boundary-value problem. To solve this boundary-value problem using the shooting method, the correct initial conditions must be determined so that the problem can be solved as an initial-value problem. Only one initial condition (σ_r) needs to be set since the other can be calculated using Eq. (12).

Determining the correct radial stress at the core is accomplished using a one dimensional optimization technique. This technique systematically reduces the design variable's initial interval of uncertainty to a desired interval where the merit function is at an extreme (maximum or minimum) value. In this case, the design variable is σ_r at the core. The merit function is the square of the radial stress at the roll's outer surface (r = c):

$$M = \left[\sigma_r(r = c)\right]^2 \tag{14}$$

Since the merit function is always positive, the desired interval of uncertainty is determined by evaluating where the merit function is a minimum to be consistent with Eq. (13).

The golden section search method was chosen as it reduces the interval of uncertainty while utilizing every merit function evaluation. This makes it a highly efficient optimization technique.

The numerical integration method used to solve each initial-value problem is a fourth order Runge-Kutta method with automatic error checking. The automatic error checking feature automatically reduces the step size to meet a desired prescribed level of accuracy.

RESULTS

This section discusses the experimental data obtained by Swanson (1991) and the stresses predicted by the nonlinear model. Swanson (1991) wound 152.4 mm (6 in) wide rolls of PET film, newsprint, and bond paper. Both Force Sensing Resistors (FSRs) and pull tabs were inserted in the rolls during winding to measure the pressure at three radial locations on the left and right side of each roll.

The wound roll parameters and material properties of the PET, bond paper, and newsprint rolls are shown in Table 1. All the rolls were wound using constant tension. Swanson (1991) wound FSRs and pull tabs into rolls at different radial locations to measure inter-layer radial pressures. FSRs are thin, flexible, resistance sensors which change resistance with applied pressure. Their application as a viable tool for measuring inter-layer pressures in wound rolls was investigated and confirmed by Fikes (1988).

Pull tabs used by Swanson (1991) consisted of two strips of thin steel feeler gauge inserted end to end in an envelope of brass shim stock. A hand held force gauge was used to measure the force required to initiate slippage of the steel feeler gauge tab in the brass envelope.

Swanson (1991) calibrated the FSRs and pull tabs in an Instron testing machine to obtain pressure values from the resistance and force data respectively. There is large variation in the pressure data which is most probably attributed to the effect of cross-web thickness variation on the FSRs. Fikes (1988) showed the resistance across the FSR can vary by as much as 150% when the load is not centered on the sensor. Since the wound roll model assumes a web of uniform thickness, the model's predicted radial stresses are compared to the average of the left and right side data.

PET film

The model calculations for wound rolls of PET film are now presented. The predicted radial stresses are compared to the in-roll radial stress data measured by Swanson (1991). First the soft initial behavior of the stack is discussed. Then an analytical method of eliminating this initial softness is presented followed by the actual model predictions.

Figure 2 shows the stress-strain relationship from stack test where a stack of the PET being wound is under uniaxial compression. The stack appears to be softer at low stresses then stiffens as the stress increases. This nonlinear behavior is most probably due to inter-layer air effects and contact asperities.

The model is provided with a means to reduce or eliminate the very soft initial data by placing the origin of the strain versus stress curve at different locations on the data. For each new origin location, $(\sigma_0, \varepsilon_0)$, the stress-strain curve is obtained from the original stack test data using the following transformations:

$$\begin{aligned} \sigma' &= \sigma - \sigma_0 \\ \varepsilon' &= \varepsilon - \varepsilon_0 \end{aligned} \tag{15}$$

The adjusted stack test data for PET is curve fitted with the function of the type described in Eq. (2). The constants k_1 through k_5 were evaluated by the least squares method for origins placed at σ_0 of 69.0, 172.4, 344.8, and 689.5 KPa. For σ_0 of at

least 172.4 KPa, just one exponential term is sufficient to fit the data. Figure 3 shows the stress-strain relationship of a PET stack corresponding to placing the origin at a magnitude of 344.8 KPa.

Using analytical expressions of the type in Eq. (2) for the original stack test data, the model did not converge on a radial stress distribution that made physical sense. The radial stress at the roll's outer surface was actually greater in magnitude than at the core, which violates the outer free surface boundary condition, and the hoop stress was negative. This suggests that the soft region of the stack test dominates the stack's stress-strain behavior. The roll is so soft that the web's decrease in hoop strain in the roll due to radial displacement is more than the hoop pre-strain, causing the residual hoop strain to be negative in the outermost wrap.

The theoretical model converged for origins at magnitudes of 68.95 KPa and higher. The in-roll stresses corresponding to placing the origin at a magnitude of 68.95, 172.4, 344.8, and 689.5 KPa are shown in Figs. 4 and 5. Figure 4 shows the predicted in-roll hoop stress profiles. Figure 4 shows that for a "soft" roll, the hoop stress is positive at the core. However, as more of the initial "soft" stack test data is eliminated, the hoop stress at the core goes negative and increases in magnitude. Since the radial stresses are greater in magnitude also, the layers squeeze down harder on the layers near the core, causing them to go into circumferential compression.

Figure 5 shows the predicted radial stress profiles. With the origin at 68.95 KPa, the radial stress is maximum at the core and decreases to zero at the outer roll surface. This is quite different from the experimental data obtained by Swanson (1991). The data shows the pressure as increasing from the core into the roll before decreasing as the roll's outer surface is approached. This is encouraging as this adjusted stack test data may still exhibit some air entrainment effects causing the stack to be somewhat soft compared to the core. Therefore, the shape of the pressure profile for this case is to be expected.

The radial stress profile starts to resemble the experimental data in both magnitude and shape when the origin is placed at 172.4 KPa. The maximum radial stress is now not at the core but at a location in the roll. The magnitude of the radial stresses are higher because the roll is stiffer as more of the assumed air effect is eliminated. The root mean square error is used to quantitatively indicate the agreement between the calculated radial stresses and experimental data. The root mean square error is 110.3 KPa.

The in-roll radial stresses corresponding to placing the origin at a magnitude of 344.8 KPa fit the experimental data best. The root mean square error between the predicted radial stresses and experimental data is 43.44 KPa.

The in-roll radial stresses corresponding to placing the origin at a magnitude of 689.5 KPa are larger than the experimental data, and the root mean square error is 158.6 KPa.

Piper (1994) showed the predicted in-roll radial stresses are larger than the experimental data with a root mean square error of 276 KPa when the origin is placed at a location where the original stack test data exhibits a more linear character.

These results show that the predicted in-roll radial stresses agree best with the experimental data when the origin of the stack test data is placed at 344.8 KPa. Figure 6 illustrates how this "best fit" solution compares with Hakiel's (1985) model. Note that Hakiel's predicted radial stresses were obtained directly from Swanson (1991) at the specific radial locations. The root mean square error between Hakiel's predicted radial

stresses and the experimental data is 1.172 MPa.

Newsprint

Like the analysis for the PET, the model was run with sections of the stack test data eliminated. A curve was fitted to the stack test data with origin locations of 34.48, 68.95, 137.9, and 206.9 KPa.

For the original stack test data and the origin at 34.48, 68.95, and 137.9 KPa, the model did not converge on a solution that made physical sense. In all cases, the radial stress at the outer surface was greater than at the core, which violates the roll's outer free surface boundary condition, and the hoop stress was negative.

Placing the origin at 206.9 KPa, the solution converged. The corresponding in-roll stresses are shown in Figures 7 and 8. The hoop stresses are slightly negative in the middle region of the roll. The radial stresses are significantly lower in magnitude than the experimental data. However, the shapes seem to be similar. Piper (1994) showed the in-roll stresses for a linear stack stress vs. strain curve are similar to those in Figs. 7 and 8.

Figure 8 shows the model developed in this thesis is no better than Hakiel's (1985) model at predicting the in-roll radial stresses for newsprint. However, the experimental data is bounded below by the model developed in this work and above by Hakiel's (1985) model.

Bond paper

Like the analysis for PET and newsprint, the model was run for wound rolls of bond paper with sections of the stack test data eliminated. For the origin at 34.48, 68.95, and 137.9 KPa, the solution did not converge as in the case of the original stack test data

For the origin at 275.8 KPa, the solution converged. The predicted hoop stress profile for bond paper is similar in shape to newsprint as shown by Piper (1994). The corresponding in-roll radial stresses are shown in Fig. 9. The root mean square error between the predicted radial stresses and the experimental data is 82.74 KPa. Figure 9 shows the model's radial stress predictions compared to Hakiel's (1985). Hakiel's (1985) model produces superior results for this material. The root mean squared error between Hakiel's predicted radial stresses and the experimental data is 48.27 KPa. However, as for newsprint, the experimental data is bounded by both models.

Piper (1994) showed that for the origin in the linear region of the original stack test data, the in-roll stresses are similar to those with the origin placed at 275.8 KPa.

CONCLUSIONS

This section summarizes the work conducted and presents the conclusions drawn from this work.

A non-linear, orthotropic model has been developed based on Umanskii's linear model. This model uses the non-linear stress-strain relationship of a stack to represent the roll's radial stress-strain behavior. A linear combination of a straight line and two exponential functions were found to describe the strain as a function of stress of a stack. The best curve fit was determined using the least squares method. The function was

found to fit the stack test data of all three materials tested: PET, bond paper, and newsprint.[5] The fitted curve was within 1% of the data for all three materials.

In-roll stress profiles were generated for PET, bond paper, and newsprint rolls using the non-linear model. The radial stress profiles were compared to experimental data obtained by Swanson (1991) who wound FSRs and pull tabs into the rolls. For all three materials, some portion of the stack test data had to be eliminated to obtain a solution that made physical sense. This gives credence to Forrest (1993) who contends that stack tests should be conducted in a vacuum chamber to reduce the inter-layer air effect.

For PET, good agreement with the experimental data was obtained when the stack test data below 344.8 KPa was eliminated. Placing the origin in the linear region worked as well as the nonlinear model for newsprint and bond paper. For newsprint, the Umanskii-based models predicted radial stresses about 20% of the experimental data. For bond paper, the Umanskii-based models predicted radial stresses about 30% of the experimental data.

Based on the limited data set for the PET rolls analyzed, placing the origin of the stack test data at approximately the radial stress at the core appears to produce the best agreement between the Umanskii-based non-linear model and experimental data. However, eliminating the non-linear region of the stack test altogether still lead to substantially under-predicting the stresses measured in the paper rolls.

The best prediction obtained from the new Umanskii-based model for a PET roll was substantially better than that provided by the Hakiel (1985) model. However, the Hakiel model worked as well as the new non-linear model for newsprint and outperformed the new non-linear model for bond paper. Nevertheless, the Hakiel model and the new non-linear model provided approximately equally spaced upper and lower bounds for both paper rolls. Thus the results of this study would indicate that both models may have commercial value.

ACKNOWLEDGMENTS

I would like to thank Dr. Thomas R. Chase of the University of Minnesota for his guidance and assistance throughout this study. My sincerest thanks also to 3M Company for their support, in particular Mary R. Hable and Dr. Albert E. Seaver for their assistance and encouragement, and Ronald P. Swanson for his insight and experimental data which proved invaluable.

REFERENCES

1. Altmann, H.C., 1968, "Formulas for Computing the Stresses in Center-Wound Rolls," The Journal of the Technical Association of the Pulp and Paper Industry, Vol. 51, No. 4, pp. 176-179.

2. Fikes, M., 1988, "The Use of Force Sensing Resistors to Measure Radial Inter-layer Pressures in Wound Rolls," (Master's Thesis), Oklahoma State University, Stillwater, Oklahoma.

3. Forrest, A.W., 1993, "A Mathematical and Experimental Investigation of the Stack Compression of Films," Proceedings of the Second International Web Handling Conference, Stillwater, Oklahoma, June 6-9.

[5]These curve fits were further adjusted to reduce initial stack softness effects.

4. Gerald, F.C., Wheatley, P.O., 1994, Applied Numerical Analysis, Fifth Edition, Addison-Wesley Publishing Company, pp. 260-271, 467-479, 490-497.

5. Hakiel, Z., 1985, "Nonlinear Model for Wound Roll Stresses," Technical Association of the Pulp and Paper Industry, Vol. 70, No. 5, pp. 113-117.

6. Piper, C.A., 1994, "A Nonlinear Model to Calculate the Stressed State of a Center-Wound Roll," (Master's Thesis), University of Minnesota, Minneapolis, Minnesota.

7. Swanson, R.P., 1991, "Determination of Wound Roll Structure Using Time of Flight Measurement," (Master's Thesis), Oklahoma State University, Stillwater, Oklahoma.

8. Timoshenko, S., 1976, Strength of Materials Part 1 - Elementary Theory and Problems, Robert Krieger Publishing Company, Inc., pp. 205-210.

9. Umanskii, E.S., Kryuchkov, V.V., and Rakovskii, V.A., 1978, "Determination of the Stressed State of a Coil of Magnetic Tape," Strength of Materials, Vol. 10, No. 3, pp. 322-335.

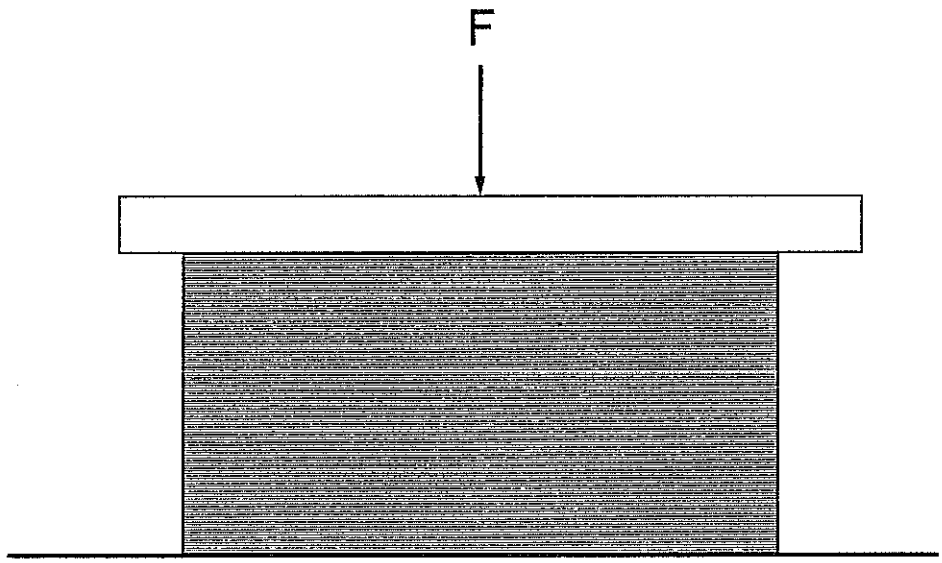

Fig.1 Stack test configuration

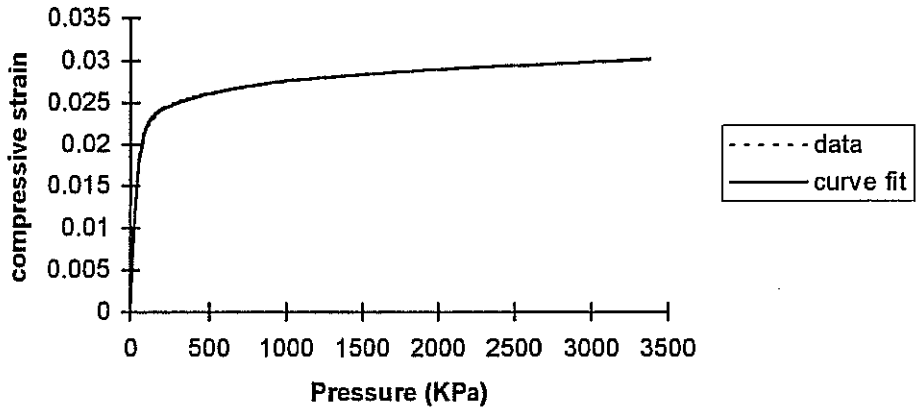

Fig. 2 PET stack test data and fitted curve
(Experimental data from Swanson, 1991)

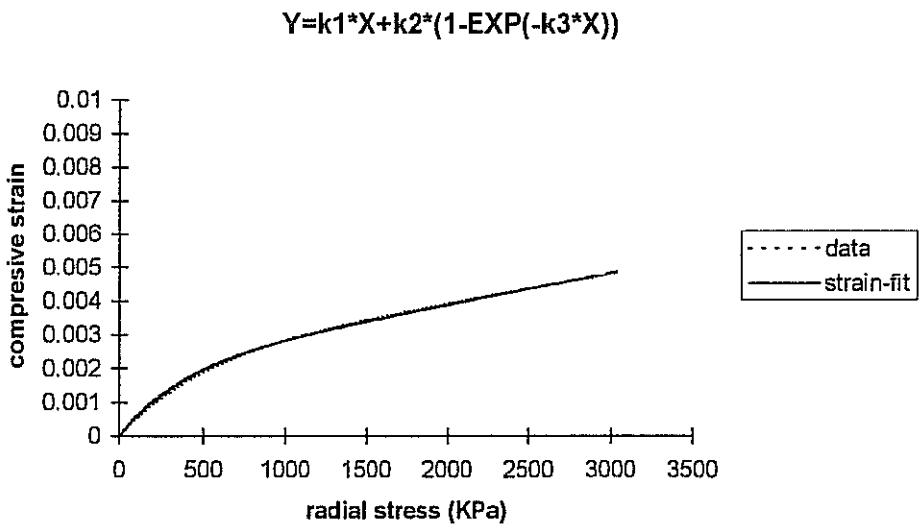

Fig. 3 PET stack test data and curve fit for σ_0 = 344.8 KPa

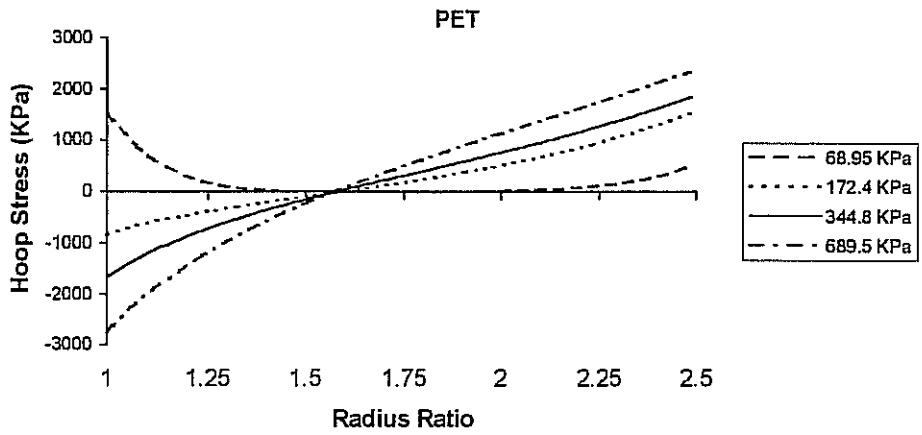

Fig. 4 Predicted hoop stress calculations for PET with σ_0 = 68.95, 172.4, 344.8, and 689.5 KPa

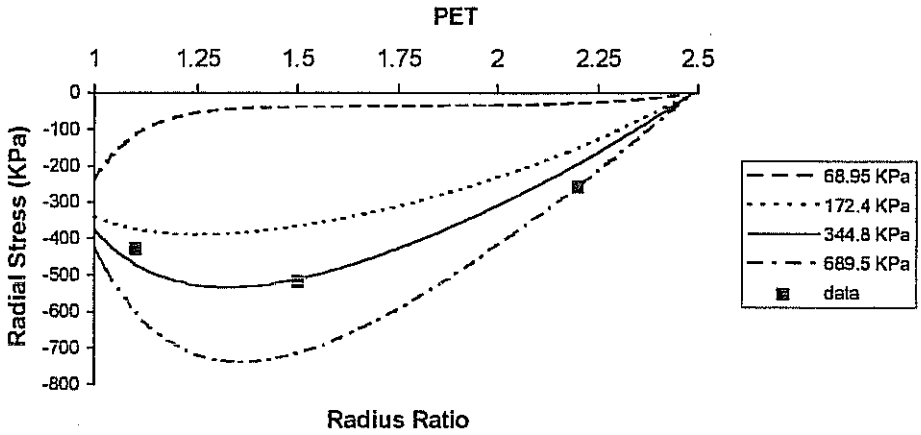

Fig. 5 Predicted radial stress calculations for PET with σ_0 = 68.95, 172.4, 344.8, and 689.5 KPa

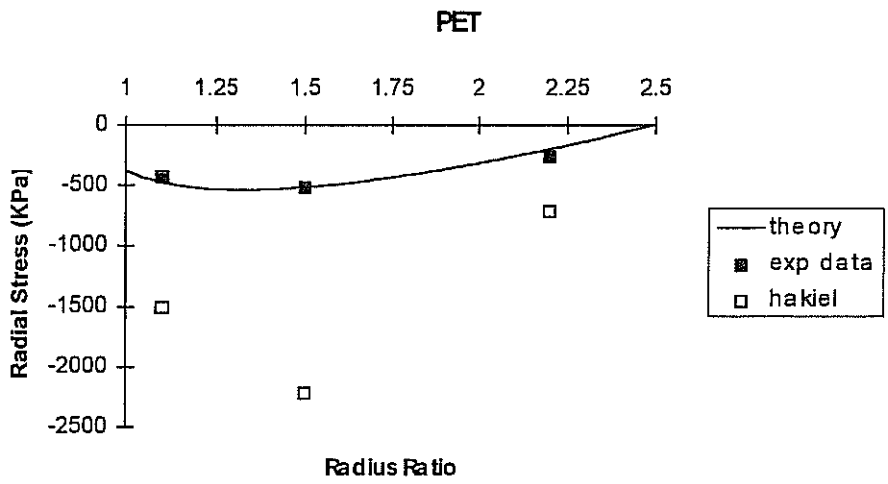

Fig. 6 Predicted radial stress for PET compared to Hakiel (1985). Hakiel's data is taken directly from Swanson (1991).

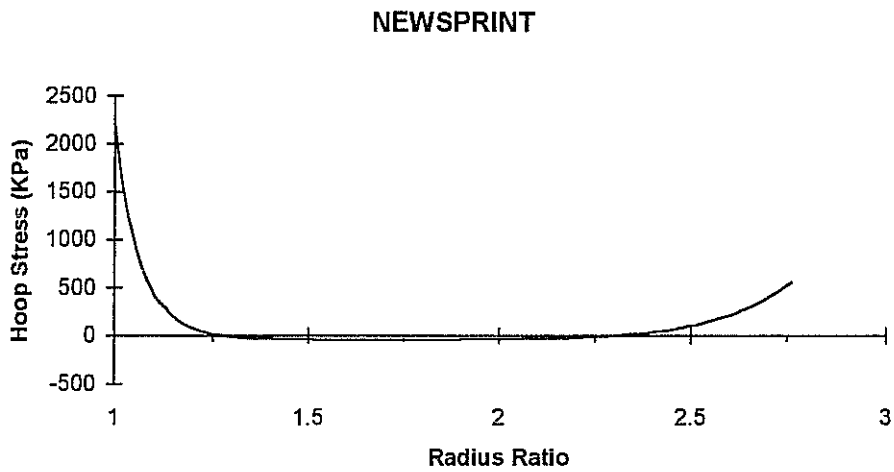

Fig. 7 Predicted hoop stresses for newsprint with σ_0 = 206.9 KPa .

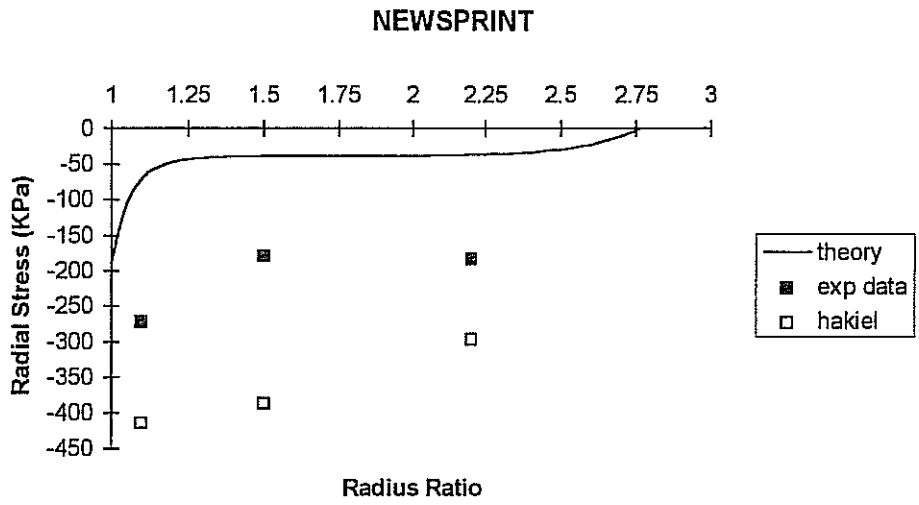

Fig. 8 Predicted radial stresses for newsprint compared to Hakiel (1985). Hakiel's data is taken directly from Swanson (1991).

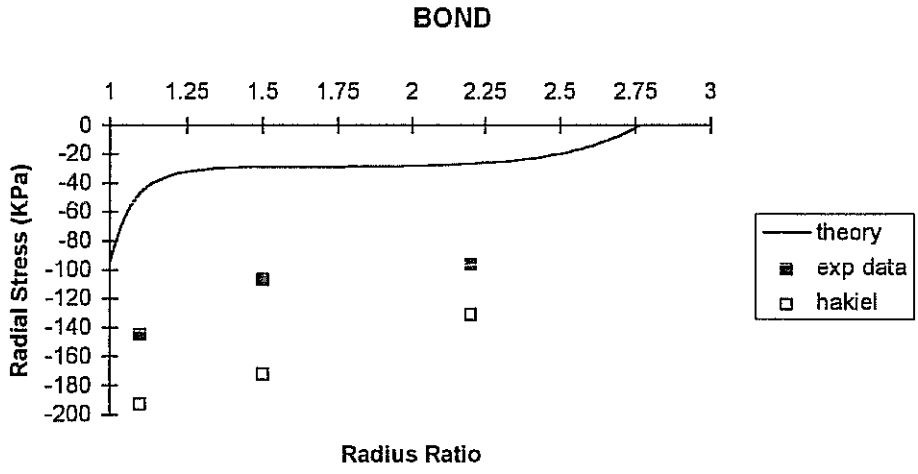

Fig. 9 Predicted radial stresses for bond paper compared with Hakiel's model. Hakiel's data is taken directly from Swanson (1991).

PET	a = 38.1 mm (1.5 in)	b = 45.97 mm (1.81 in)
	c = 114.3 mm (4.5 in)	$\upsilon_{er} = 0.3$
	$E_\theta = 3.07$ GPa	$\sigma_w = 6.895$ MPa
	$E_h = 689.5$ MPa	$\upsilon_h = 0.33$
Newsprint	a = 38.1 mm (1.5 in)	b = 45.97 mm (1.81 in)
	c = 127 mm (5.0 in)	$\upsilon_{er} = 0.3$
	$E_\theta = 3.37$ GPa	$\sigma_w = 6.895$ MPa
	$E_h = 689.5$ MPa	$\upsilon_h = 0.33$
Bond paper	a = 38.1 mm (1.5 in)	b = 45.97 mm (1.81 in)
	c = 127 mm (5.0 in)	$\upsilon_{er} = 0.3$
	$E_\theta = 3.82$ GPa	$\sigma_w = 3.45$ MPa
	$E_h = 689.5$ MPa	$\upsilon_h = 0.33$

Table 1. Wound roll properties (from Swanson, 1991).

Piper, C.
A Nonlinear Model to Calculate the Stressed State of a Center-Wound Roll
6/19/95 Session 1 10:45 - 11:10 a.m.

Question - You use significant cropping of your data and I just wanted to point out that if you use the energy solution method the energy under the curve is very small at those low levels and it does come out in the solution, so you can use the stack test data directly and you don't have to manipulate it by cropping it artificially. That's another approach you might want to consider in your work. Also, the Umanskii model the first curves you showed of it showed that it predicted only 25 percent tension in the outer rack as anyone who has done winding knows there is significant tension in the outer wrap all you need to do is slice that wrap off with a razor cut and you will see it spring apart; that's known as the Cameron Gap Test to the old people in the industry, but its well known that a significant amount of tension is contained in the outer wrap, so I'm a little curious as to whether the Umanskii model is valid for that reason.

Answer - I haven't looked at any literature that presents the actual tension in the outer wrap. That's something that if I'm looking at this model further, I would do.

Question - Chris one thing I noted in your paper, you blame some of the none correlation, if you will, between data and model on air entrainment, as I read the paper I couldn't get a good grasp of what sort of air entrainment would be expected in your experimental tests. There were no winding velocities I saw no roughness for the PET and for the newsprint and this sort of thing; and quit frankly you've really got to wind newsprint reasonable fast to really get some air entrainment effects into it because the air permeates out through the substrate. I guess what sort of velocity were you winding at or what was Ron winding at.

Answer - This experimental data was taken by Ron Swanson, it was work he did at OSU, Ron is also an employee of 3M, as far as I understand that was a 50 to 100 ft per minute range which is in the 15 to 16 to 30 meters per minute per range. I guess if you look at entrapped air during winding its a function of velocity and radius of the surface roughness, wouldn't think that air entrainment would be important under those winding conditions, it wouldn't be dominant.

Question - Well you say that's the predominate difference why the model does not meet the experiment data. Ron's in the audience, do we know what that Web was? It was a polyester, was it a 3M polyester?

Answer - No.

Comment - So it was either the 442 or 377 or the S, one of those, OK very good. As well as the winding velocity in things that were used, right? 100 feet per minute; very good.

Thank you.